Identifying the Molecular Origin of Global Warming[†]

Partha P. Bera,[‡,||] Joseph S. Francisco,[§] and Timothy J. Lee*,[‡,⊥]

NASA Ames Research Center, Space Science and Astrobiology Division, Moffett Field, California 94035, and Department of Chemistry and Department of Earth and Atmospheric Sciences, Purdue University, West Lafayette, Indiana 47907-1393

We have investigated the physical characteristics of greenhouse gases (GHGs) to assess which properties are most important in determining the efficiency of a GHG. Chlorofluorocarbons (CFCs), hydrofluorocarbons (HFCs), perfluorocarbons (PFCs), nitrogen fluorides, and various other known atmospheric trace molecules have been included in this study. Compounds containing the halogens F or Cl have in common very polar X−F or X−Cl bonds, particularly the X−F bonds. It is shown that as more F atoms bond to the same central atom the bond dipoles become larger as a result of the central atom becoming more positive. This leads to a linear increase in the total or integrated X−F bond dipole derivatives for the molecule, which leads to a nonlinear (quadratic) increase in infrared (IR) intensity. Moreover, virtually all of the X−F bond stretches occur in the atmospheric IR window as opposed to X−H stretches, which do not occur in the atmospheric window. It is concluded that molecules possessing several F atoms will always have a large radiative forcing parameter in the calculation of their global warming potential. Some of the implications for global warming and climate change are discussed.

Introduction

Global climate change is regarded as one of the most significant scientific challenges to address in the coming decades. Temperature equilibrium in the Earth's atmosphere is maintained by a balanced absorption and emission of all the electromagnetic radiation reaching the surface of the Earth. Over the last few decades, an increasing trend in the global surface temperature has been caused, at least in part, by an increased concentration of greenhouse gases (GHG). Gases in the atmosphere play a vital role in maintaining this delicate temperature balance.

Carbon dioxide, methane, nitrous oxide, hydrofluorocarbons (HFC), chlorofluorocarbons (CFC), and perfluorocarbons (PFC) are the most common anthropogenic greenhouse gases. Carbon dioxide gets wide attention due to its rapidly increasing concentration in the atmosphere. Methane, although a trace gas having a relatively short average lifetime of 12 years in the atmosphere, is a much more potent greenhouse gas compared to CO_2. The concentration of CH_4 in the atmosphere has been on the rise at an average rate of 8.9 ppbv/year for the last two decades.[1] Nearly 45% of the methane released into the atmosphere is done so by anthropogenic activities, including agriculture and domestic activities. The rest comes from natural sources such as wasteland decomposition and termites. With increasing global temperatures, the methane release rate is expected to increase causing a positive feedback loop for global warming. When all effects are included, it is estimated that 0.48 Wm^{-2} radiative forcing comes from methane alone, which is almost a third of that for CO_2, although one recent study on methane radiative forcing based on an emissions-based approach suggests that this may underestimate the actual impact by almost

a factor of 2.[2,3] Likewise, another naturally occurring greenhouse gas, nitrous oxide, is about 200 times more potent compared to CO_2. N_2O is produced during the burning of fossil fuels and is also released by the soil.[4] Furthermore, in a recent study by Shine and Sturges, it is estimated that 40% of the heat trapped by anthropogenic greenhouse gases in the Earth's atmosphere is due to gases other than CO_2.[5]

Other potent greenhouse gases, such as hydrofluorocarbons (HFCs), chlorofluorocarbons (CFCs), and perfluorocarbons (PFCs), are heavily used in the electronics, air conditioning, appliances, and carpet manufacturing industries. Production and industrial use of CFCs have been discontinued since it was discovered that they contribute to the destruction of the ozone layer. However, PFCs and HFCs are continually utilized in various industries. In addition to the above uses, PFCs are used as a blood substitute in biological cell cultures and in blood transfusions.[6] PFCs are also widely used as tracers in atmospheric studies, in tracking leaks in gas lines and electrical transmission lines,[7] and in tracking carbon sequestration processes.[8] Although the current concentration of some of these tracer gases has been found to be very small compared to that of CO_2, their concentration is on the rise for as long as the data exist.[9] More importantly, PFCs and HFCs are extremely efficient greenhouse gases as they absorb in the atmospheric infrared window and in some cases have atmospheric lifetimes estimated at thousands of years.[2] This means that some PFCs and HFCs display the characteristics to impact global temperatures significantly more than CO_2 in terms of both short-term and long-term effects. Although it is estimated that they contribute little to the total radiative forcing at present, with the current rate of increase they will be significant contributors in the future according to some models.[5] Some hydrofluoroethers have been suggested as substitutes for CFCs and HFCs, as carrier compounds for lubricants, and for use in the refrigeration industry. Although the hydrofluoroethers have slightly lower atmospheric lifetimes due to reactions with the OH radical and

Identifying the Molecular Origin of Global Warming

J. Phys. Chem. A, Vol. 113, No. 45, 2009 **12695**

other atmospheric scrubbing agents, they have a relatively large radiative efficiency.[10]

An index was introduced some years ago to quantify the potency of an individual molecule regarding global warming.[11] This index, the "Global warming potential" (GWP), is defined as the time-integrated radiative forcing of one gas with respect to a reference gas over a time horizon. The absolute GWP depends on the time horizon for which the GWP is considered. However, it is pointed out in chapter 6 of the Intergovernmental Panel on Climate Change (IPCC) working group's 2001 report[12] that the GWP of a molecular species is relatively insensitive to the choice of the time horizon when the atmospheric lifetime of the gas is not substantially different from the response time of the reference gas (for CO_2, this is about 150 years[12]). The GWP of different molecules can vary significantly. For example, over a 100 year time horizon, the GWP of CH_4 is 25 times and N_2O is 298 times the GWP of CO_2, while the GWP of CFC-11 (CCl_3F) is 4750 times that of CO_2.[2] It is clear that GWP is a quantity that is very specific to a molecular species and that, while atmospheric lifetime is a factor, a molecule's radiative efficiency is often the deciding factor for large variations in GWPs.

The relative radiative forcing parameter is determined on a molecule per molecule basis compared to a reference, usually CO_2.[2] Generally, a radiative transfer model is used to determine the radiative forcing for perturbations of greenhouse gases. In these computations, a certain concentration of a perturbing gas along with the molecule's infrared profile (absorption bands and strengths) is added to the model. From a molecular standpoint, the radiative efficiency depends on the total absorption of electromagnetic radiation by a molecule, especially within the so-called atmospheric window. While it is established that the radiative efficiency can vary significantly for different molecular species, the underlying chemical or physical causes for this variation have not been studied. That is, the GWP of different greenhouse gases measured over the same time horizon can vary significantly due to their inherent chemical natures. The purpose of the present research is to identify the underlying molecular properties that cause GWPs to vary so much among different types of molecules. If one is to minimize the impact of anthropogenic materials on global climate change, it is necessary to design better materials that have minimal absorption capabilities in the atmospheric window or shorter atmospheric lifetimes. A number of studies have addressed how to minimize the atmospheric lifetime of materials;[13,14] however, no studies have addressed how to minimize the absorption capabilities of molecular species in the atmospheric window. In the present report, we present new insights into how properties of a molecule influence the molecular absorption in the atmospheric window and the underlying molecular cause of global warming. Theoretical methods used in the present study are detailed in the next section, followed by the Results and Discussion, and then Conclusions in the final section.

Theoretical Methods

The determination of equilibrium structures for all molecules was performed using the second-order Moller–Plesset perturbation theory (MP2) in conjunction with a double-ζ plus polarization and diffuse function basis set denoted DZP++ (indicating that diffuse functions are included on hydrogen atoms).[15–18] All ab initio electronic structure calculations were performed with the Q-Chem3.1[19] quantum chemistry program. Harmonic vibrational frequencies and infrared (IR) intensities were computed using the same level of theory. The IR vibrational intensities

were computed using the double harmonic approximation (i.e., mechanical and electrical harmonicity). Under the double harmonic approximation, infrared vibrational intensities are proportional to the square of the dipole derivatives.[20] The Cartesian dipole derivatives obtained at the MP2/DZP++ level of theory have been transformed into the simple internal coordinates for each molecule to assess various molecular properties. For simplicity, the simple internal coordinates used are limited to the bond distances and angles of the molecules concerned. Intder 2005,[21] a code for vibrational analysis and nonlinear transformations of quartic force fields (including property force fields), has been used to transform the Cartesian dipole derivatives into simple internal coordinate derivatives.

Results and Discussion

Although carbon dioxide, methane, and nitrous oxide are considered to be the main greenhouse gases, as discussed in the Introduction, there are others, especially the halocarbons. One interesting question then is what are the common dominating factors or collection of factors that make certain molecules effective greenhouse gases and others ineffective? Our initial investigation led to the first observation: certain bond stretch vibrational modes are ideally suited for occurring in the atmospheric IR window region (for purposes of this study, we have defined the atmospheric IR window to be $800-1400$ cm^{-1}). These modes include C–F, C–Cl, C–Br, S–F, and N–F vibrational stretches among other vibrational modes. Some bond angle bending and torsions fall within the atmospheric window and contribute to global warming albeit in a significantly lesser way for reasons that will be discussed below.

To investigate further, collected in Table 1 are the summed IR intensities of several GHGs plus some other atmospheric trace molecules of interest. Also included is the summed IR intensity for bands that occur in the atmospheric window and the percentage of the total IR intensity that contributes to the bands occurring in the atmospheric window. The atmospheric lifetime and the GWPs (for a time horizon of 100 years) are taken from ref 9.[12] It is evident that some of the most effective GHGs have GWPs that are thousands of times that of CO_2. In fact, CFCs, which fall into this category, have been recommended for use in the Martian atmosphere to keep Mars warm and habitable.[22] A systematic inspection into the IR vibrational frequencies and intensities of some of the most common HFCs and CFCs listed in Table 1 has led to the following conclusions: (1) the IR absorption intensities within the IR atmospheric window are much larger than that of CO_2, and therefore they are much more potent absorption agents than CO_2; and (2) the percentage of the integrated vibrational absorption intensity that falls within the atmospheric window increases, up to as high as 99% of the total IR intensity, as more and more halogens are involved. These factors, boosted by very long atmospheric lifetimes, contribute to making the HFCs, CFCs, PFCs, and other GHGs extremely potent compared to CO_2 on a per molecule basis. The data reported in Table 1 highlight that it is not only the fact that these molecules possess long atmospheric lifetimes but also, even more important, their inherent capability to strongly absorb radiation in the atmospheric window that make them worthy of attention. The HFCs, CFCs, PFCs, and sulfur and nitrogen fluorides not only absorb in the atmospheric window, where no other atmospheric molecules absorb, but also do so very effectively. The fact that for many of these molecules more than $85-90\%$ of their IR absorption occurs in the atmospheric window was perhaps not well understood or not well appreciated.

TABLE 1: Atmospheric Lifetimes, Global Warming Potentials (GWP), Integrated Infrared Absorption Intensities, Integrated Infrared Intensities in the Atmospheric IR Window, and the Percent IR Intensity in the Atmospheric Window for Some Common Greenhouse Gases

industrial name	chemical name	lifetime years	GWP 100 year	int. IR intensity km mol^{-1}	intensity in atmospheric window km mol^{-1}	%
water	H_2O			159.0	0.0	0.0
carbon dioxide	CO_2	100[a]	1	594.5	25.7	4.1
nitrous oxide	N_2O	114	298	351.3	13.6	3.88
methane	CH_4	12	25	127.5	44.1	34.6
methyl fluoride	CH_3F	2.6	97	241.1	119	49.4
HFC-32	CH_2F_2	4.9	675	535.6	406.3	75.9
HFC-23	CHF_3	270	14800	947.6	759.6	80.2
PFC-14	CF_4	50000	7390	1419.6	1403	98.8
CFC-13	$CClF_3$	640	14400	1225.63	1199	97.9
CFC-12	CCl_2F_2	100	10900	979.79	970.1	99.0
CFC-11	CCl_3F	45	4750	707.4	705.2	99.7
methyl chloride	CH_3Cl	1	13	109	26	23.9
methylene chloride	CH_2Cl_2	0.38	8.7	198.7	168.5	84.8
chloroform	$CHCl_3$	0.5	30	333.7	327.6	98.2
carbon tetrachloride	CCl_4	26	1400	443.73	443.7	99.9
methyl bromide	CH_3Br	0.7	5	80.3	40.7	50.7
HCFC-22	$CHClF_2$	12	1810	769.3	742	96.5
ammonia	NH_3			278.02	217	78.0
nitrogen trifluoride	NF_3	740	17200	519.9	516.2	99.3
sulfur hexafluoride	SF_6	3200	22800	554.2	434	78.3
SF_5CF_3	SF_5CF_3	>1000	18000	2029.5	1823	89.8
sulfur dioxide	SO_2			172.36	137.1	79.5
phosphine	PH_3			303.92	64.77	21.3
trifluorophosphine	PF_3			662.46	619.8	93.6
ozone	O_3			1802.2	1.69	0.1
oxygendifluoride	OF_2			76.44	75.91	99.3

[a] http://cdiac.ornl.gov/pns/current_ghg.html.

TABLE 2: MP2/DZP++ Harmonic Vibrational Frequencies (ω in cm^{-1}) and IR Intensities (I in km mol^{-1}) of Some Chlorofluorocarbons, Fluorocarbons, And Nitrogen Fluorides[a]

	ω_1	I	ω_2	I	ω_3	I	ω_4	I	ω_5	I	ω_6	I	ω_7	I	ω_8	I	ω_9	I
CH_4	**1238**	**14.7**	**1238**	**14.7**	**1380**	**14.7**	1586	0	1586	0	3109	0	3268	17	3268	17	3268	17
CH_3F	**1069**	**117**	**1212**	**0.9**	**1213**	**0.9**	1521	5.3	1537	3.3	1537	3.3	3136	41.5	3260	34.3	3261	34.4
CH_2F_2	523	5.6	**1109**	**278**	**1123**	**109**	**1199**	**18.8**	**1295**	**0**	1494	35.1	1577	1.9	3186	1.9	3283	52.8
CHF_3	503	2.9	503	2.9	696	14.6	**1146**	**107**	**1176**	**327**	**1176**	**327**	1426	67.1	1426	67.1	3273	33.4
CF_4	430	0	430	0	627	5.5	627	5.5	627	5.5	**907**	**0**	**1295**	**467.7**	**1295**	**467.7**	**1295**	**467.7**
$CClF_3$	352	0.0	352	0.0	489	0.5	559	2.4	559	2.4	786	20.8	**1138**	**478**	**1223**	**361**	**1223**	**361**
CCl_2F_2	274	0.0	328	0	446	0.5	450	0.6	467	0.2	671	8.5	**962**	**370**	**1113**	**324**	**1159**	**276**
CCl_3F	258	0.1	258	0.1	366	0.1	411	0.2	411	0.2	551	1.5	**889**	**241**	**889**	**241**	**1079**	**241**
CH_3Cl	793	21.2	1067	2.4	1067	2.4	1456	17.5	1517	4.5	1517	4.5	3150	31.7	3274	12.4	3274	12.4
CH_2Cl_2	297	0.5	753	11.7	824	112	**943**	**1.1**	**1221**	**0**	**1365**	**55.1**	1506	0.3	2195	16.2	3288	1.5
$CHCl_3$	275	0.1	275	0.1	385	0.3	703	5.2	**824**	**134**	**824**	**134**	**1293**	**30.3**	**1293**	**30.3**	3245	0.4
CCl_4	232	0	232	0	33	0.1	331	0.1	331	0.1	478	0	**827**	**148**	**827**	**148**	**827**	**148**
NH_3	**1063**	**217**	1695	25.2	1695	25.2	3559	2.0	3732	4.3	3732	4.3						
NH_2F	**956**	**28.3**	**1282**	**76.9**	**1343**	**1.3**	1643	36.8	3509	1.1	3636	2.5						
NHF_2	496	2.4	**915**	**161**	**996**	**31.7**	**1347**	**47.5**	**1471**	**20.8**	3494	2.2						
NF_3	489	0.7	489	0.7	646	2.4	**910**	**236**	**910**	**236**	**1038**	**44.4**						

[a] Bold indicates that the band occurs in the atmospheric window. See text for details.

Comparison of the total IR intensity occurring within the atmospheric window for similar F and Cl containing molecules contained in Table 1 (e.g., CF_4 vs CCl_4 or CHF_3 vs $CHCl_3$) shows that F containing molecules are much more effective greenhouse gases compared to Cl containing molecules. In addition, we note that the molecule with the largest total IR intensity in the atmospheric window is SF_5CF_3 (1823 km mol^{-1}), and while SF_6 has a total IR intensity of 434 km mol^{-1} in the atmospheric window, it is much smaller in comparison. Of the molecules included in Table 1, only three molecules have a total IR intensity in the atmospheric window greater than 1000 km mol^{-1}—CF_4 (1403), $CClF_3$ (1199), and SF_5CF_3 (1823)—but considering that the total IR intensity in the atmospheric window for CO_2, CH_4, and N_2O is only 25.7, 44.1, and 13.6 km mol^{-1},

respectively, even the compounds with total IR intensity in the atmospheric window in the hundreds of kilometers per mole are significant greenhouse gases.

A systematic study of the HFCs and PFCs (see Table 2) reveals that with introduction of each F atom more and more vibrational modes occur in the atmospheric window by virtue of the C–F bond stretch falling within the 800–1400 cm^{-1} region, while simultaneously each C–F stretch is becoming more intense. Figure 1 shows graphically that as one introduces F, going from CH_4 to CF_4, the percentage of the total amount of IR intensity within the atmospheric window increases from 20% up to almost 100%. It is important to emphasize that simultaneously the absolute IR intensity of the C–F stretches increases along this series. For example, the IR intensity per
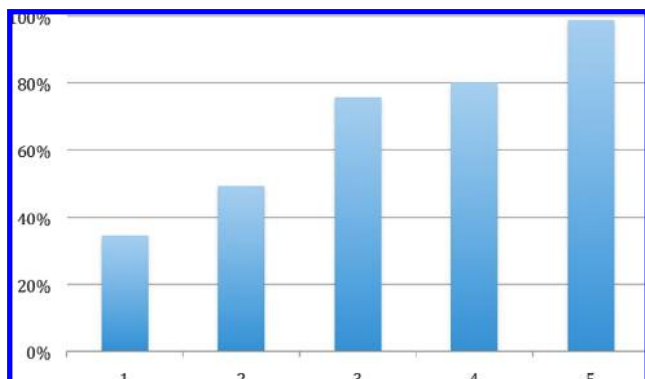
Identifying the Molecular Origin of Global Warming

J. Phys. Chem. A, Vol. 113, No. 45, 2009 **12697**

Figure 1. Percent integrated infrared intensities in the atmospheric IR window of (1) CH$_4$, (2) CH$_3$F, (3) CH$_2$F$_2$, (4) CHF$_3$, and (5) CF$_4$.

C−F bond in the CH$_3$F to CF$_4$ series is 117, 193.5, 253.7, and 350.8 km mol^{-1}, respectively (see Table 2).

Under the double harmonic approximation, a vibrational band IR intensity is proportional to the square of the dipole derivative. Therefore, a large intensity is the manifestation of a larger dipole derivative. The dipole derivatives calculated for some GHGs in the simple internal coordinate system are presented in Table 3. For a systematic test of the above we computed the dipole derivatives of the C−H, C−F, C−Cl, and N−F bonds for a series of molecules in the simple internal coordinate system. For the CH$_4$, CH$_3$F, CH$_2$F$_2$, CHF$_3$, and CF$_4$ series, the individual dipole derivatives increase at first and then decrease slightly. However, the integrated dipole derivative increases linearly as seen in Figure 2a. On going from CH$_4$ to CH$_3$F to CH$_2$F$_2$, the dipole derivative increases due to a greater electronegativity difference between C/F compared to C/H. However, the dipole derivative does not increase as one might have expected, and in fact it decreases on going from CH$_2$F$_2$ to CHF$_3$ to CF$_4$. This can be rationalized by looking at Figure 3. Each additional F renders the central C more positive. As the ionic character or the oxidation state of the central C increases, so does its electron-attracting ability, i.e., electronegativity. Therefore, as the central C becomes more cationic in nature, its absolute electronegativity

increases, and the electronegativity difference between it and the terminal fluorines decreases. The smaller electronegativity difference yields smaller dipole derivatives. However, the integrated dipole derivatives for the C−F stretching modes increase across the entire series as seen in Figure 2a. Likewise, the dipole derivatives increase on going from NH$_3$ to NH$_2$F to NHF$_2$ to NF$_3$ (see Figure 2b). Figures 2b and 2d show that the integrated IR intensities increase even more rapidly across both series due to the fact that they are proportional to the square of the dipole derivatives.

Fluorine, being strongly electronegative, forms very polar bonds with the central atom whether that be C or N. Each additional F atom makes the central atom more positively charged by drawing electronic charge away, making all of the C−F or N−F bonds more and more polar across the series. We have attempted to quantify this effect by computing a "bond dipole" using either Mulliken populations[23] or the natural population analysis (NPA).[24] These are collected in Table 3 together with the percent IR intensity in the atmospheric window from Table 1, for comparison. We note that the electrostatic interaction between the central atom, which is positively charged, and the negatively charged terminal fluorine also causes gradual bond shortening. The bond shortening acts as a mitigating factor for the bond dipole. Hence, although elec-tronegativity difference between the central and the terminal atoms qualitatively decide the ionic nature of the bond, it is hardly the only contributing factor.[25] Mulliken qualitatively broke down the dipole moment of a bond into four components: primary, overlap, hybridization, and core.[26] The primary moment originates due to electronegativity difference between atoms. While the electronegativity difference is one of the contributing factors to the overall asymmetry in the electronic cloud of the bond, other factors can also contribute and are sometimes dominant. Therefore, an attribution of a trend in the dipole derivatives or even the bond dipoles to merely electronegativity differences of the atoms involved would be an oversimplifica-tion. Nevertheless, electronegativity differences play a vital role in creating asymmetry in the electronic environment of a bond and in the case of the X−F bonds studied here is the dominant contribution to the bond dipole. To summarize, the highly

TABLE 3: Dipole Derivatives and NPA Bond Dipole Moments and Mulliken Bond Dipole Moments of Selected HFCs, PFCs, and CFCs

| industrial name		dipole derivative Debye/Å		NPA bond dipole		Mulliken bond dipole		% intensity in IR window
carbon dioxide	CO$_2$	CO	5.540	CO	2.314	CO	1.283	4.1
		OCO	1.354					
nitrous oxide	N$_2$O	NN	2.844	NN	0.690	NN	0.586	3.88
		NO	5.900	NO	1.134	NO	0.903	
methane	CH$_4$	CH	0.725	CH	0.525	CH	0.377	40.4
methyl fluoride	CH$_3$F	CF	4.660	CF	−0.520	CF	−0.397	49.4
HFC-32	CH$_2$F$_2$	CF	5.242	CF	−1.408	CF	−1.079	75.9
HFC-23	CHF$_3$	CF	5.218	CF	−2.164	CF	−1.499	80.2
PFC-14	CF$_4$	CF	4.710	CF	−2.872	CF	−1.922	98.8
CFC-13	CClF$_3$	CF	5.055	CF	−2.034	CF	−0.113	97.9
		CCl	2.883	CCl	−0.647	CCl	0.196	
CFC-12	CCl$_2$F$_2$	CF	5.216	CF	−1.436	CF	−0.618	99.0
		CCl	3.239	CCl	−1.682	CCl	−0.627	
CFC-11	CCl$_3$F	CF	5.248	CF	−0.792	CF	−0.113	99.7
		CCl	3.348	CCl	−0.647	CCl	0.196	
methyl chloride	CH$_3$Cl	CCl	2.121	CCl	0.475	CCl	1.010	23.9
methylene chloride	CH$_2$Cl$_2$	CCl	3.101	CCl	0.730	CCl	0.949	84.8
trichloromethane	CHCl$_3$	CCl	3.309	CCl	0.528	CCl	0.949	98.2
carbon tetrachloride	CCl$_4$	CCl	3.356	CCl	0.081	CCl	0.344	99.9
ammonia	NH$_3$	NH	0.248	NH	0.881	NH	0.626	78.0
nitrogen dihydrofl	NH$_2$F	NF	3.220	NF	0.243	NF	0.112	72.5
difluoro	NHF$_2$	NF	4.329	NF	−0.599	NF	−0.526	90.5
nitrogen trifluoride	NF$_3$	NF	4.863	NF	−1.230	NF	−0.942	99.3
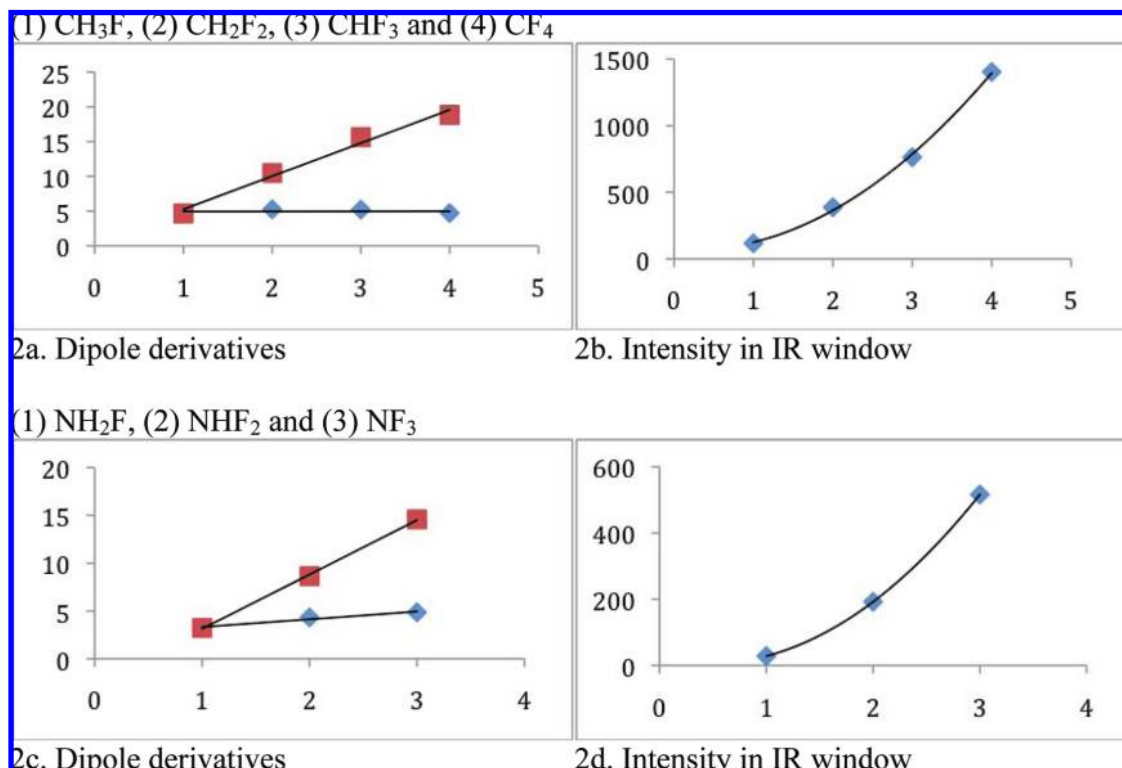
Figure 2. (a) Blue data points are dipole derivatives of each C–F bond in CH$_3$F, CH$_2$F$_2$, CHF$_3$, and CF$_4$. Red data points are cumulative dipole derivatives for the same series of molecules. (b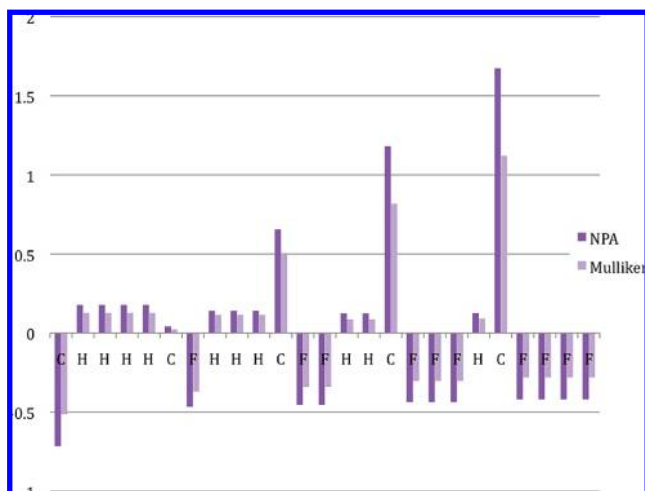) Integrated infrared absorption intensity in the IR window. (c) Blue data points are individual dipole derivatives of each N–F bond in NH$_2$F, NHF$_2$, and NF$_3$. Red data points are cumulative dipole derivatives for a given molecule. (d) Integrated infrared absorption intensity in the IR window.

Figure 3. Natural population charges and Mulliken atomic charges on each atomic center of CH$_4$, CH$_3$F, CH$_2$F$_2$, CHF$_3$, and CF$_4$.

polarized nature of the X–F bond leads to a large dipole derivative; increasing the number of fluorine atoms bonded to a given central atom increases the total or integrated dipole derivative linearly as a function of the number of F atoms, leading to a nonlinear increase in IR intensity. Therefore, a combination of factors, (1) the X–F stretching frequencies falling within the atmospheric IR window; (2) the strong electronegativity of F; and (3) the typically long atmospheric lifetimes of compounds containing many fluorine atoms (since they do not usually readily react with OH) contribute toward making fluorine-containing compounds the most effective global warming agents.

Conclusions

As a rule of thumb, a large atomic electronegativity leads to polar bonds by drawing charge from its bonding partner. The total bond polarity or the bond dipole moment increases as the electronegativity difference increases, and a larger bond dipole yields a larger bond dipole derivative leading to a large IR intensity. The total or integrated IR intensity for a given molecule, however, depends on the number of polar bonds, as well as the polarity of each bond. Therefore, since fluorine is highly electronegative, molecules containing several fluorine atoms are strong greenhouse gases and are much more effective warming agents compared to equivalent Cl and/or H containing species. With the addition of each F, the integrated bond dipole derivative for the molecule increases linearly, and hence the total IR absorption intensity increases dramatically. Moreover, the increased IR absorption contributes to a molecule's radiative forcing since the C–F stretching frequencies occur in the atmospheric window. In summary, large dipole derivatives for the vibrational modes that fall within the atmospheric IR window yield very large integrated IR intensities for the HFCs, PFCs, and CFCs—sometimes an order of magnitude more than that of the common greenhouse gases like CO$_2$, O$_3$, N$_2$O, and CH$_4$. The insights developed in this study should help in better understanding the physical characteristics of greenhouse gases and specifically what makes an efficient greenhouse gas on a molecular level. It is hoped that the results from this study will be used in the design of more environmentally friendly materials.

Identifying the Molecular Origin of Global Warming

J. Phys. Chem. A, Vol. 113, No. 45, 2009 **12699**

References and Notes

(1) Wuebbles, D. J.; Hayhoe, K. *Earth-Sci. Rev.* **2002**, *57*, 177.

(2) Forster, P.; Ramaswamy, V.; Artaxo, P.; Berntsen, T.; Betts, R.; Fahey, D. W.; Haywood, J.; Lean, J.; Lowe, D. C.; Myhre, G.; Nganga, J.; Prinn, R.; Raga, G.; Schulz, M.; Dorland, R. v. Changes in Atmospheric Constituents and in Radiative Forcing. In *Climate Change 2007: The Physical Science Basis. Contribution of Working group I to the Fourth Assessment Report of the Intergovernmental Panel on Climate Change*; Solomon, S., Qin, D., Manning, M., Chen, Z., Marquis, M., Averyt, K. B. M. T., Miler, H. L., Eds.; Cambridge University Press: Cambridge, United Kingdom and New York, NY, USA, 2007.

(3) Shindel, D. T.; Faluvegi, G.; Bell, N.; Schmidt, G. A. F. L.-C. I. O. *Geophys. Res. Lett.* **2005**, *32*, L04803.

(4) Bateman, E. J.; Baggs, E. *Biol. Fertil. Soils* **2005**, *41*, 371.

(5) Shine, K. P.; Sturges, W. T. *Science* **2007**, *315*, 1804.

(6) Spence, R. K. *Artif. Cells. Blood Substitutes Immobilization Biotechnol.* **1995**, *23*, 367.

(7) Hassoun, S.; McBride, T.; Russel, D. A. *J. Environ. Monit.* **2000**, *2*, 432.

(8) White, C. M.; Strazisar, B. R.; Granite, E. J.; Hoffman, J. S.; Pennline, H. W. *J. Air Waste Manage. Assoc.* **2003**, *53*, 645.

(9) Watson, T. B.; Wilke, R.; Dietz, R. N.; Heiser, J.; Kalb, P. *Environ. Sci. Technol.* **2007**, *41*, 6909.

(10) Oyaro, N.; Sellevag, S. R.; Nielsen, C. J. *Environ. Sci. Technol.* **2004**, *38*, 5567.

(11) Hammitt, J. K.; Jain, A. K.; Adams, J. L.; Wuebbles, D. J. *Nature* **1996**, *381*, 301.

(12) Ramaswamy, V.; Boucher, O.; Haigh, J.; Hauglustaine, D.; Haywoood, J.; Myhre, G.; Nakajima, T.; Shi, G. Y.; Solomon, S.; Betts, R.; Charlson, R.; Chuang, J. S.; Daniel, A.; Del Genio, A.; Dorland, R. v.; Feichter, J.; Fuglestvedt, S.; Forster, P.; Ghan, S. J.; Jones, A.; Kiehl, J. T.; Koch, D.; Land, C.; Lean, J.; Lohman, U.; Minscheaner, K.; Penner, J. E.; Roberts, D. L.; Rodhe, H.; Roelofs, G. J.; Rotstayan, L. D.; Schneider, T. L.; Schumann, U.; Schwartz, S. E.; Schwarzkopf, M. D.; Shine, K. P.; Smith, S.; Stevenson, D. S.; Stordal, F.; Tegen, I.; Zhang, Y., *Climate Change 2001: The Scientific Basis. In Climate Change 2001*; Houghton, J. T., Ding, Y., Griggs, D. J., Noguer, M., Linden, P. J. v. d., Dai, X., Maskell, K., Johnson, C. A., Eds.; Cambridge University Press: Cambridge, 2001.

(13) (WMO), W. M. O. "Scientific Assesment of Ozone Research and Monitoring Project - Report No. 37," 1995.

(14) Clam, J. M.; Didion, D. A. Trade-offs in refrigerant Selections: Past, Present, and Future; *ASHRAE/NIS, Refrigerant Conference, Refrigerant for the 21st Century*, 1997, Gaithersburg, MD.

(15) Dunning, T. H. *J. Chem. Phys.* **1970**, *53*, 2823.

(16) Dunning, T. H. *J. Chem. Phys.* **1971**, *55*, 3958.

(17) Huzinaga, S. *J. Chem. Phys.* **1962**, *42*, 1293.

(18) Lee, T. J.; Schaefer, H. F. *J. Chem. Phys.* **1985**, *83*, 1784.

(19) Shao, Y.; Molnar, L. F.; Jung, Y.; Kussmann, J.; Ochsenfeld, C.; Brown, S. T.; Gilbert, A. T. B.; Slipchenko, L. V.; Levchenko, S. V.; O'Neill, D. P.; DiStasio, R. A.; Lochan, R. C.; Wang, T.; Beran, G. J. O.; Besley, N. A.; Herbert, J. M.; Lin, C. Y.; Van Voorhis, T.; Chien, S. H.; Sodt, A.; Steele, R. P.; Rassolov, V. A.; Maslen, P. E.; Korambath, P. P.; Adamson, R. D.; Austin, B.; Baker, J.; Byrd, E. F. C.; Dachsel, H.; Doerksen, R. J.; Dreuw, A.; Dunietz, B. D.; Dutoi, A. D.; Furlani, T. R.; Gwaltney, S. R.; Heyden, A.; Hirata, S.; Hsu, C. P.; Kedziora, G.; Khalliulin, R. Z.; Klunzinger, P.; Lee, A. M.; Lee, M. S.; Liang, W.; Lotan, I.; Nair, N.; Peters, B.; Proynov, E. I.; Pieniazek, P. A.; Rhee, Y. M.; Ritchie, J.; Rosta, E.; Sherrill, C. D.; Simmonett, A. C.; Subotnik, J. E.; Woodcock, H. L.; Zhang, W.; Bell, A. T.; Chakraborty, A. K.; Chipman, D. M.; Keil, F. J.; Warshel, A.; Hehre, W. J.; Schaefer, H. F.; Kong, J.; Krylov, A. I.; Gill, P. M. W.; Head-Gordon, M. *Phys. Chem. Chem. Phys.* **2006**, *8*, 3172.

(20) Gussoni, M.; Zerbi, G.; Person, W. *Pure Appl. Chem.* **1988**, *60*, 1385.

(21) Allen, W. D. Intder2005 is a general program written by W. D. Allen and co-workers, which performs vibrational analysis and higher order nonlinear transformations, 2005.

(22) Gerstell, M. F.; Francisco, J. S.; Yung, Y. L.; Boxe, C.; Aaltonee, E. T. *Proc. Natl. Acad. Sci.* **2001**, *98*, 2154.

(23) Szabo, A.; Ostlund, N. S. *Modern Quantum Chemistry: Introduction to Advanced Electronic Structure Theory*; Dover: New York, 1998.

(24) Reed, A. E.; Curtiss, L. A.; Weinhold, F. *Chem. Rev.* **1988**, *88*, 899.

(25) Smyth, C. P. *J. Phys. Chem.* **1955**, *59*, 1121.

(26) Mulliken, R. S. *J. Am. Chem. Soc.* **1950**, *72*, 4493.